Science Bulletin xxx (xxxx) xxx

Contents lists available at ScienceDirect

Science Bulletin

journal homepage: www.elsevier.com/locate/scib

Science Bulletin
www.scibull.com

Article

CVD growth of perovskite/graphene films for high-performance flexible image sensor

Kailun Xia [a], Wenqiang Wu [b,c], Mengjia Zhu [a], Xinyi Shen [d], Zhe Yin [a], Haomin Wang [a], Shuo Li [a], Mingchao Zhang [a], Huimin Wang [a], Haojie Lu [a], Anlian Pan [c,*], Caofeng Pan [b,*], Yingying Zhang [a,*]

[a] Key Laboratory of Organic Optoelectronics and Molecular Engineering of Ministry of Education, Department of Chemistry, Tsinghua University, Beijing 100084, China
[b] CAS Center for Excellence in Nanoscience, Beijing Key Laboratory of Micro-Nano Energy and Sensor, Beijing Institute of Nanoenergy and Nanosystems, Chinese Academy of Sciences, Beijing 100083, China
[c] Key Laboratory for Micro-Nano Physics and Technology of Hunan Province, State Key Laboratory of Chemo/Biosensing and Chemometrics and College of Materials Science and Engineering, Hunan University, Changsha 410082, China
[d] Cavendish Laboratory, University of Cambridge, Cambridge CB3 0HE, UK

ARTICLE INFO

Article history:
Received 17 September 2019
Received in revised form 3 November 2019
Accepted 6 December 2019
Available online xxxx

Keywords:
Hybrid perovskite
Chemical vapor deposition
Graphene template
Flexible photodetector array
Artificial retina

ABSTRACT

Hybrid perovskite possesses excellent photoelectric properties, including large light-absorption capacity and high carrier mobility, and is an ideal light-absorbing material for photoelectric devices. The grain size and compactness of hybrid perovskite are key factors affecting the performance of photoelectric devices. The photocurrent and photoresponsivity of these devices are relatively low because of the rapidly recombined photoexcited electron-hole pairs in hybrid perovskite. Herein, we develop a facile two-step chemical vapor deposition (CVD) method to synthesize a high-quality van der Waals (vdWs) $MAPbI_3$/graphene heterostructure for high-performance image sensor. We introduced inorganic sources (PbI_2) to vdWs epitaxially grown PbI_2 film on a seamless graphene monolayer film template through CVD. Methylammonium iodide (MAI) was then reintroduced to prepare the vdWs $MAPbI_3$/graphene heterostructure. The $MAPbI_3$ layer is composed of densely packed, large-size grains and displays a smooth surface. High photoresponsivity of 10^7 A/W is achieved in the corresponding photodetector. Inspired by the human visual system, we designed a flexible photodetector array containing (24×24) pixels, achieving perfect image recognition and color discrimination. Our study may greatly facilitate the construction of high-performance optoelectronic devices in artificial retina, biomedical imaging, remote sensing, and optical communication.

1. Introduction

Photodetector, which converts light into electrical signals has been widely used in industries and science, including sensing and communication [1–4]. Its key component is the light-absorbing material. In particular, hybrid perovskite (e.g., methylammonium halide lead ($MAPbX_3$, X = Cl, Br, I)) has recently received extensive attention [5–9] and possesses excellent photoelectric properties, including large light-absorption capacity, high carrier mobility, suitable band gap and long electron-hole diffusion length, making it an ideal light-absorbing material for photodetector [10–13]. However, the performance of a hybrid perovskite-based photodetector highly depends on the quality of the hybrid perovskite material, especially its grain size and film compactness. In addition, the photoexcited electron-hole pairs in the hybrid perovskite recombine within a few picoseconds (i.e., within the lifetime of photoexcited electrons), thereby reducing photocurrent and photoresponsivity [5,14–16]. Therefore, preparing high-quality perovskite and improving the deficiency of the hybrid perovskite itself are necessary to obtain a high-performance photodetector.

Van der Waals (vdWs) heterostructure, which is prepared through the construction of materials and interfaces, can be used to improve light-substance interactions to build high-performance photoelectric devices [17–19]. Graphene has received great attention due to its unique properties [20], including high mobility, broadband absorption, and fast response time, thereby enabling its enormous application potential in photonics and optoelectronics [21–23]. When graphene and hybrid perovskite form a vdWs heterostructure, the empty state in the hybrid perovskite

* Corresponding authors.
E-mail addresses: anlian.pan@hnu.edu.cn (A. Pan), cfpan@binn.cas.cn (C. Pan), yingyingzhang@tsinghua.edu.cn (Y. Zhang).

https://doi.org/10.1016/j.scib.2019.12.015
2095-9273/

Please cite this article as: K. Xia, W. Wu, M. Zhu et al., CVD growth of perovskite/graphene films for high-performance flexible image sensor, Science Bulletin, https://doi.org/10.1016/j.scib.2019.12.015

valence band produced through photon absorption will be filled by the electrons in the proximal graphene layer. Therefore, the recombination of photoexcited electron-hole pairs in the hybrid perovskite is reduced, and the electrons remain in the conduction band without being attenuated [5,14]. Furthermore, the graphene surface has no dangling bonds, in which sp^2-hybridized carbon atoms are closely packed into a two-dimensional (2D) honeycomb lattice. Owing to the low energy barrier of epitaxial growth, graphene can be used as an ideal template to facilitate the vdWs epitaxial growth of 2D materials and consequently enable the synthesis of high-quality hybrid perovskite films [24–27]. Therefore, the presence of graphene can produce high-quality perovskite, improve the interface light-substance interaction, and boost the photocurrent and performance of photodetectors.

In this work, we developed a facile two-step CVD method to prepare a high-quality vdWs $MAPbI_3$/graphene heterostructure and verify its application for image sensors. The hybrid perovskite was synthesized on a seamless monolayer graphene film by sequentially introducing inorganic sources (PbI_2) and organic sources (methylammonium iodide, MAI) through CVD. The seamlessly large-area grain-boundary-free graphene film was grown by CVD and used as a growth template. The vdWs epitaxially grown hybrid perovskite layer is dense and smooth and possesses large-size grains. Basing on the vdWs $MAPbI_3$/graphene heterostructure, we constructed a photodetector and obtained an extremely high photoresponsivity of ~10^7 A/W and a low response time of 50 ms. Inspired by the human visual system, we also designed an integrated (24 × 24) pixels flexible photodetector array as an image sensor, in which the vdWs $MAPbI_3$/graphene heterostructure was used as cone cells. We demonstrated the photon detection, resolution of the color and clear shape imaging of the flexible image sensor. The high-quality vdWs $MAPbI_3$/graphene heterostructure has extensive application potentials in integrated optoelectronic circuits, biomedical imaging, and optical communication in the future.

2. Materials and methods

2.1. Synthesis of high-quality seamless monolayer graphene films

The monolayer graphene film was synthesized on copper (Cu) foil (25 μm thick, Alfa Aesar Inc.) by CVD. The Cu foil was cleaned in hot acetic acid for 30 min to remove the surface oxides and impurity, and then washed with acetone, isopropanol and deionized (DI) water for 10 min, respectively. The cleaned Cu foil was dried with a nitrogen gun. We placed the Cu foil into the center of the furnace and then heated to 1070 °C with a flow of hydrogen (H_2, 100 sccm (standard cubic centimeter per minutes), 99.999% purity) and Ar (500 sccm, 99.999% purity) in 50 min. This system was kept for 5 h and then methane (CH_4) (0.2 sccm, 99.999% purity) was introduced. The growth was terminated after 50 min by stopping the CH_4 flow and then cooled down the system in Ar and H_2.

2.2. Transfer of graphene

The transfer process was as follows: (1) Spin coating 300 nm polymethyl methacrylate (PMMA, 3000 r/min for 30 s) on the graphene/Cu surface; (2) bake the sample in thermal drying oven at 170 °C for 10 min; (3) put the sample into $(NH_4)_2S_2O_8$ solution (0.5 mol/L) to etch the Cu foil; (4) pick up the floating PMMA/graphene film with a clean glass slide and wash in deionized water for 3 times; (5) dry in a blast oven for 30 min to remove water; (6) dip into acetone to dissolve the PMMA layer.

2.3. Synthesis of PbI_2 films on monolayer graphene film templates

PbI_2 powder (98%, J&K Chemicals) was used as the inorganic source and was put into a quartz tube. The graphene template substrate was put into the downstream region of the tube. The quartz tube was first evacuated to a pressure of 3 Pa and then Ar (200 sccm) was introduced. Ten minitues later, the furnace was heated to 320 °C and held for another 10 min. Finally, the furnace was cooled down naturally with flowing Ar to ambient temperature.

2.4. Synthesis of $MAPbI_3$ films on monolayer graphene film templates

CH_3NH_3I powder (99.999%, J&K Chemicals) was used as the organic source and was put into a quartz tube. The PbI_2/graphene substrate was put into the downstream region. The quartz tube was first evacuated to a pressure of 3 Pa and then Ar (200 sccm) was introduced. Ten minitues later, the furnace was heated to 180 °C and held for another 30 min. Finally, the furnace was cooled down naturally with flowing Ar to ambient temperature. The obtained sample was annealed at 100 °C in air for 50 min for crystal transformation.

2.5. Fabrication of flexible photodetector array

The fabrication process was as follows: (1) Spin coat a layer of NR9-3000PY type negative photoresist on cleaned PET film. After photoetching, deposit 50 nm Au as the X-direction electrode. (2) Spin coat a layer of AZ601 type positive photoresist on the sample of (1). After photoetching, deposit 100 nm alumina as the insulating layer. (3) Spin coat a layer of AZ601 type positive photoresist on the sample of (2). After photoetching, deposit 50 nm Pt as the Y-direction electrode. (4) Transfer a layer of graphene on the sample of (3) and then spin coat a layer of AZ601 type positive photoresist. After photoetching, etch graphene. (5) Spin coat a layer of AZ601 type positive photoresist on the sample of (4) and then grow PbI_2 crystals in a CVD system. (6) Remove the photoresist with acetone and left PbI_2/graphene film on the substrate. (7) Synthesis $MAPbI_3$ perovskite by introducing CH_3NH_3I. (8) Remove the excess CH_3NH_3I with isopropanol and then obtain the flexible photodetector array.

3. Results and discussion

3.1. Fabrication and characterization of the PbI_2 grown on monolayer graphene templates

Fig. 1a illustrates a schematic diagram of the preparation of high-quality vdWs $MAPbI_3$/graphene heterostructure on a graphene template (see details in Materials and methods). The graphene template is a seamless monolayer graphene film composed of aligned millimeter graphene domains grown on copper (Cu) foil by CVD (Fig. S1 online). The film has few cracks or defects, a dangling-bond-free surface, and a 2D honeycomb lattice. This film is the key to achieving the epitaxial growth of high-quality perovskite films. First, we introduced inorganic sources (PbI_2) to synthesize high-quality PbI_2 on graphene films. The organic sources (MAI) were reintroduced to prepare the vdWs $MAPbI_3$/graphene heterostructure according to the synthesized vdWs PbI_2/graphene heterostructure.

Fig. 1b and c show the top and side views of the lattice structure of the PbI_2/graphene heterostructure, respectively. PbI_2 has a layered crystal structure, and it is mainly the vdWs force between the PbI_2 and the graphene layer. The orientation of PbI_2 crystals is derived from the lattice-matching between graphene and PbI_2 and the relatively low total energy of the entire heterostructure

Please cite this article as: K. Xia, W. Wu, M. Zhu et al., CVD growth of perovskite/graphene films for high-performance flexible image sensor, Science Bulletin, https://doi.org/10.1016/j.scib.2019.12.015

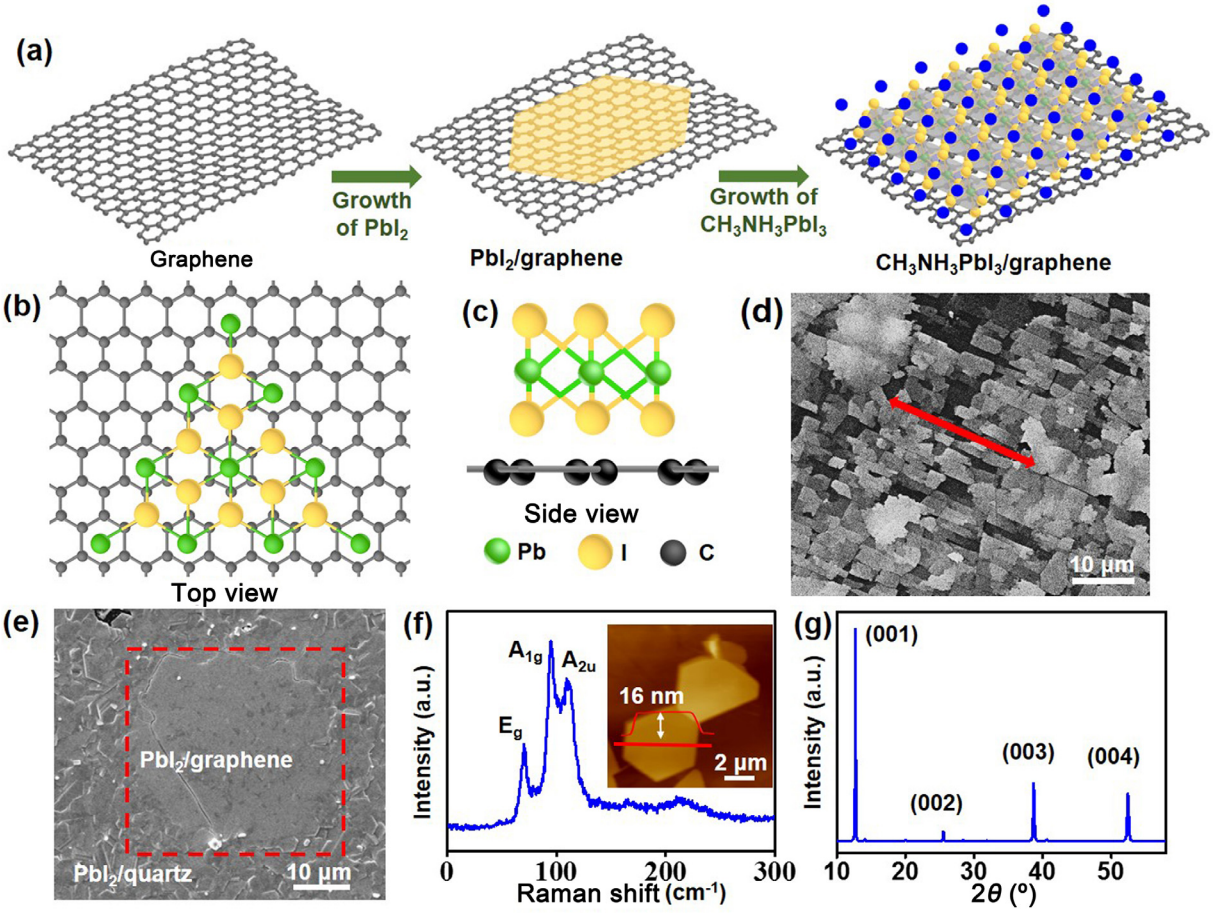

Fig. 1. (Color online) Illustration of the preparation process of vdWs high-quality $MAPbI_3$/graphene heterostructure and the structure of the PbI_2/graphene heterostructure. (a) Schematic diagram showing the preparation process of vdWs $MAPbI_3$/graphene heterostructure by sequentially introducing PbI_2 and MAI through a two-step CVD. Schematic diagram showing the lattice structure of vdWs PbI_2/graphene heterostructure in top view (b) and side view (c). (d) SEM image of incompletely filmed PbI_2 sample grown on graphene. (e) SEM image of PbI_2 film grown on a single crystal graphene domain on a quartz substrate. Raman spectrum (f) and XRD profile (g) of a PbI_2 film grown on graphene. The inset picture in (f) is an AFM topography image of PbI_2.

system [28]. Fig. 1d is a scanning electron microscope (SEM) image of the PbI_2 crystals grown on graphene showing the aligned PbI_2 crystals, indicating the potential for seamless merging. Short growth time was intentionally used for this sample to clearly show the aligned PbI_2 crystals grown on the graphene template. Fig. 1e shows a SEM image of the PbI_2 crystals grown on a single crystal graphene domain on a quartz substrate. The PbI_2 films grown on graphene films are smoother than those grown on quartz, indicating the excellent epitaxial promotion effect of the graphene templates (see details in Fig. S2 online). Furthermore, we used transmission electron microscopy (TEM), atomic force microscopy (AFM), Raman spectroscopy, and X-ray diffraction (XRD) to systematically study the structure and chemical properties of the epitaxially grown vdWs PbI_2/graphene heterostructure. Fig. 1f shows the typical Raman spectrum of the PbI_2 sample revealing three characteristic peaks, namely, E_g (75 cm^{-1}), A_{1g} (96 cm^{-1}), and A_{2u} (113 cm^{-1}). The inset picture is an AFM topography image of PbI_2 domains grown on graphene, indicating a height of ~16 nm of the PbI_2 domain. The XRD pattern of the grown PbI_2 film shows (0 0 1), (0 0 2), (0 0 3), and (0 0 4) peaks occurring on the PbI_2 film, suggesting that 2D PbI_2 domains possess the 2H hexagonal crystalline structure (Fig. 1g). A low magnification TEM image of a PbI_2 domain shows a smooth surface, and the selected area electron diffraction pattern of the PbI_2 further confirms its single-crystallinity property (Fig. S3 online).

3.2. Characterization of vdWs $MAPbI_3$/graphene heterostructures

High-quality vdWs $MAPbI_3$/graphene heterostructure films can be grown on vdWs epitaxially grown PbI_2 films. Fig. 2**a** is a SEM image of a vdWs $MAPbI_3$/graphene heterostructure showing that the film is dense, and the size of the $MAPbI_3$ crystal grains is ~2 μm. The AFM image further proves the compactness and large grain size of the film (Fig. 2b). We intentionally synthesized the $MAPbI_3$ film on quartz for comparison to verify the high-quality $MAPbI_3$ film grown on graphene template (see details in Materials and methods). Fig. 2c is a SEM image of a $MAPbI_3$ film grown directly on quartz through a two-step CVD showing that the $MAPbI_3$ film has an average grain size of ~150 nm. Fig. 2d shows an AFM topography image of a $MAPbI_3$ film grown on quartz, thereby further revealing its small grain size and porous film properties. Compared with the perovskite grown directly on the quartz substrate, the perovskite film prepared by using graphene as a template has larger crystal grains and a denser film structure, and the crystallinity of the perovskite is remarkably improved.

We used photoluminescence (PL) spectroscopy, XRD, and X-ray photoelectron spectroscopy (XPS) to further study the structure and chemical composition of the synthesized $MAPbI_3$ film. Fig. 2e is the typical PL spectra of the $MAPbI_3$ film grown on quartz and vdWs $MAPbI_3$/graphene heterostructure. It shows that the PL quenching in the vdWs $MAPbI_3$/graphene heterostructure was

Please cite this article as: K. Xia, W. Wu, M. Zhu et al., CVD growth of perovskite/graphene films for high-performance flexible image sensor, Science Bulletin, https://doi.org/10.1016/j.scib.2019.12.015

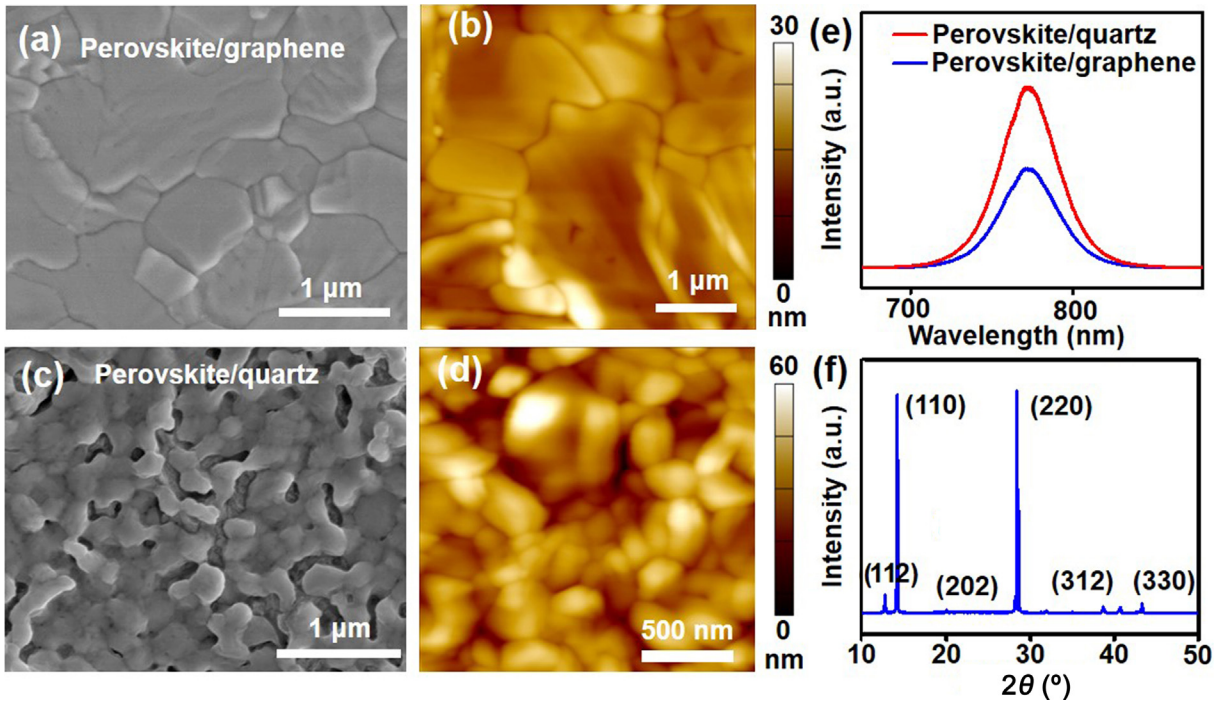

Fig. 2. (Color online) Characterization of $MAPbI_3$ grown on vdWs PbI_2/graphene heterostructures and quartz. SEM (a) and AFM (b) topography images of a vdWs $MAPbI_3$/graphene heterostructure, respectively. SEM (c) and AFM (d) topography images of a $MAPbI_3$ film grown on quartz, respectively. (e) Photoluminescence spectra of a $MAPbI_3$ film and a vdWs $MAPbI_3$/graphene heterostructure. (f) XRD pattern of a vdWs $MAPbI_3$/graphene heterostructure.

lower than that in the $MAPbI_3$ film. In the presence of graphene, the electrons in the graphene layer were transferred to the proximal hybrid perovskite layer to fill the empty state in the hybrid perovskite valence band produced by photon absorption, reducing the recombination of photoexcited electron-hole pairs in hybrid perovskite and thereby contributing to the high-performance of the photodetectors [29]. Fig. 2f shows the XRD pattern of the $MAPbI_3$ film grown on graphene. It shows diffraction peaks at 14.2°, 28.4° and 43.2°, which can be assign to the (1 1 0), (2 2 0) and (3 3 0) crystal faces of the tetragonal phase of $MAPbI_3$ and are consistent with previous results [1]. The relative intensity of the (1 1 0) and (2 2 0) peaks are very high, and the full width at half-maximum of the (1 1 0) and (2 2 0) peaks are only 0.024 and 0.016, respectively, indicating the high crystallinity of the as-grown $MAPbI_3$ film [30]. The XPS spectrum of the vdWs $MAPbI_3$/graphene heterostructure exhibited four elements, namely, C, N, I, and Pb (Fig. S4 online). The UV–visible absorption spectra of the vdWs $MAPbI_3$/graphene heterostructure showed its great light-absorption performance in the visible range (Fig. S5 online). This finding indicates that the vdWs $MAPbI_3$/graphene heterostructure can fully adsorb light energy and produce electron-hole pairs, thereby confirming its effective photodetection under visible light irradiation.

3.3. Photoelectric performance of the vdWs $MAPbI_3$/graphene heterostructure based photodetector

We constructed photodetectors based on the high-quality vdWs $MAPbI_3$/graphene heterostructure to study the photoelectric properties of the as-prepared heterostructures (Fig. 3). Fig. 3a shows the schematic configuration of the photodetector in which vdWs $MAPbI_3$/graphene heterostructure is used as a light-absorbing layer. Fig. 3b shows the photocurrent of the photodetector with different incident illumination powers under 633 nm illumination wavelength at 1 V bias. The photocurrent was linearly proportional to the incident illumination power. Fig. 3c exhibits the current–voltage (I–V) curves of the photodetector as a function of illumination wavelength with a fixed incident illumination power of 30 μW. Good light responsiveness was observed. When the illumination wavelength was close to the infrared band, the degree of light response was lowered, which corresponds to the light-absorption range of $MAPbI_3$. Fig. 3d shows the illumination power-dependent I-V curves of the photodetector under an illumination wavelength of 633 nm. The photocurrent of the device increased with the illumination power and voltage.

Photoresponsivity describes the photoelectric conversion capability of the device and is an important indicator for photodetectors that is related to the device material, illumination power, and wavelength of light. Photoresponsivity (R) can be defined as $R = (I_{light} - I_{dark})/(P_0 \times S)$, where I_{light} is the photocurrent when the light is ON, I_{dark} is the dark current when the light is OFF, P_0 is the irradiance power density, and S is the effective illuminated area. Fig. 3e shows the relationship between photoresponsivity and illumination power within a fixed wavelength of 633 nm. At 0.1 V, the photodetector exhibited an impressive photoresponsivity value of ~2700 A/W with an illumination power of 100 nW. We also prepared a photodetector based on a $MAPbI_3$ film without graphene for comparison (Fig. S6 online). The $MAPbI_3$ photodetectors showed a photoresponsivity value of ~0.2 A/W with an illumination power of 100 nW, which is significantly lower than that of the $MAPbI_3$/graphene based photodetector. It shows that a high photoresponsivity can be achieved with weak light intensity. A reduced light intensity lowers the carrier concentration in the sensitizer layer, which generally reduces the electron-hole recombination. An almost linear relation was observed between photoresponsivity and illumination power ($R \propto P^{-1}$) (Fig. S7 online). When the power was reduced to 1 pw, the photoresponsivity was ~10^7 A/W. This value is comparable or higher than that for previous $MAPbI_3$/graphene film-based photodetectors [1,5,16,29,31–39].

Furthermore, we studied the periodic response capability and flexibility of the proposed device. The photo-switching characteristics of

Please cite this article as: K. Xia, W. Wu, M. Zhu et al., CVD growth of perovskite/graphene films for high-performance flexible image sensor, Science Bulletin, https://doi.org/10.1016/j.scib.2019.12.015

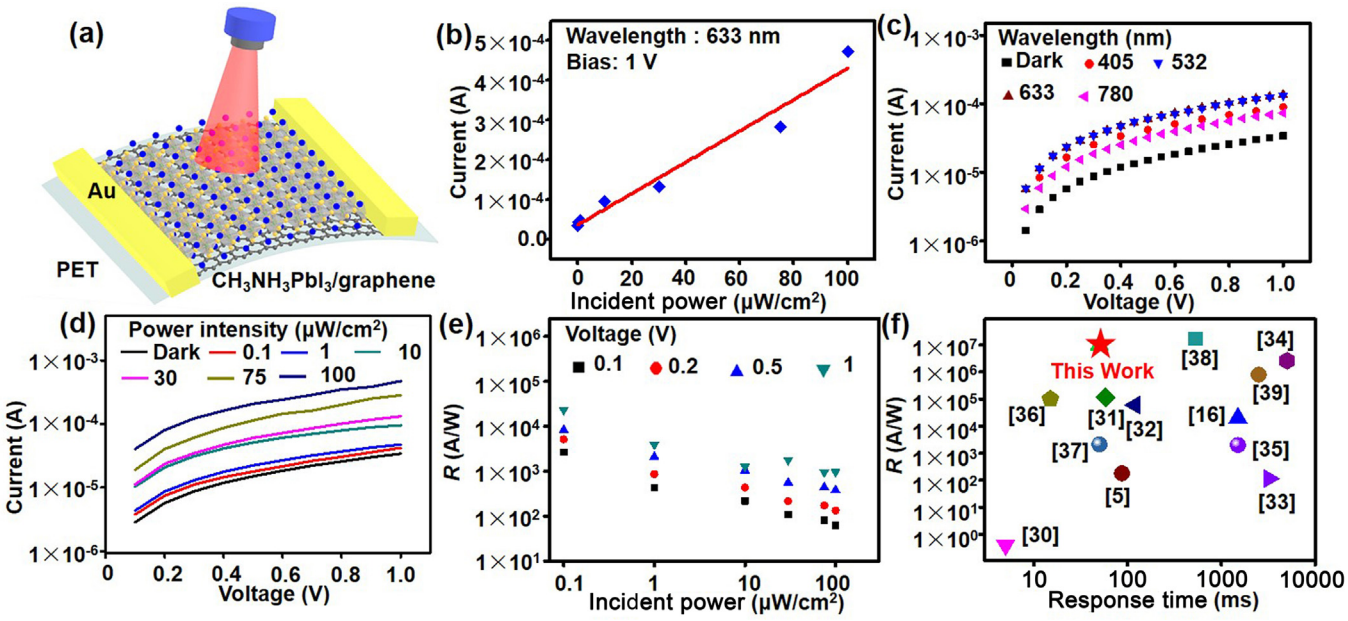

Fig. 3. (Color online) Schematic configuration and performance of the vdWs $MAPbI_3$/graphene heterostructure based photodetector. (a) Schematic diagram of the photodetector. (b) Photocurrent vs. incident illumination power under an illumination wavelength of 633 nm at 1 V bias. (c) *I-V* curves of the photodetector under various illumination wavelength. The incident illumination power is 30 μW. (d) *I-V* curves of the photodetector under various illumination power. The illumination wavelength is 633 nm. (e) Photoresponsivity of the photodetector under different voltages and illumination power. (f) Comparison of the photoresponsivity and response time of our vdWs $MAPbI_3$/graphene heterostructure based photodetector with the previous reported $MAPbI_3$/graphene film based photodetector.

the photodetector were measured under alternating light illumination (30 μW, 633 nm) with the gate and drain voltages of 0 and 0.1 V, respectively (Fig. S8 online). The device shows a stable performance with cyclic photocurrents that follow light signals. Response time is defined as the time used by the photocurrent to increase from null to 80% of the saturation level [40]. The response time was less than 50 ms, thereby indicating the rapid response of the device (Fig. S9 online). We also used a polyimide (PI) film as a flexible substrate to prepare a $MAPbI_3$/graphene heterostructure based flexible photodetector, which showed no significant performance

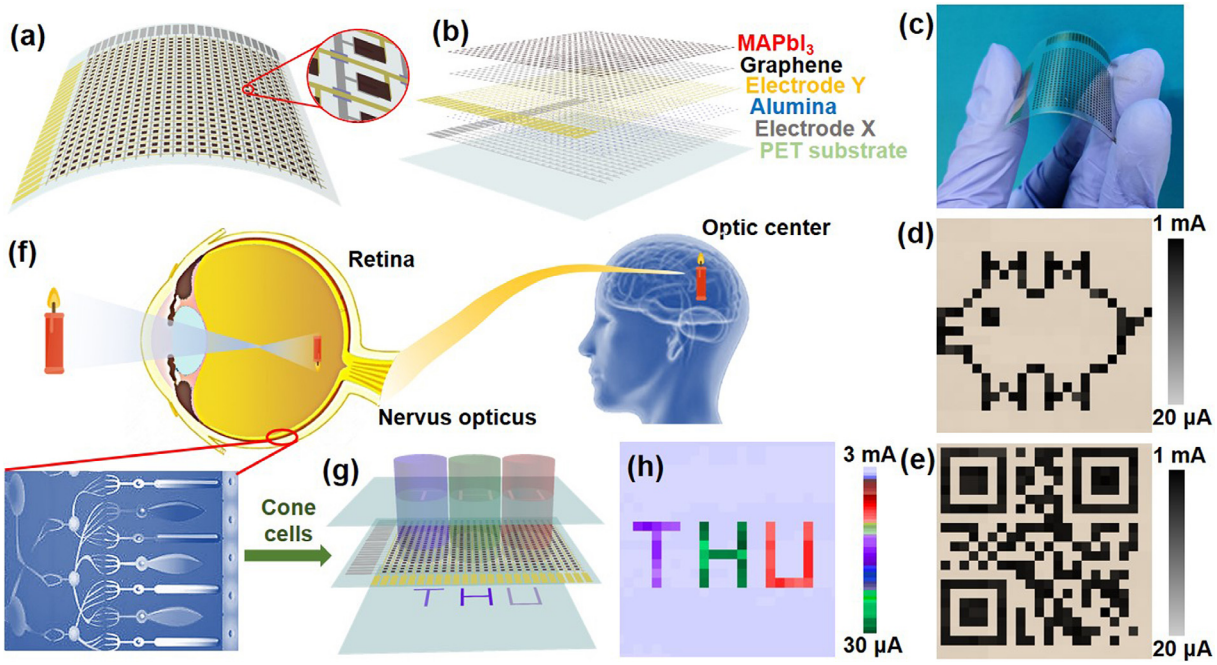

Fig. 4. (Color online) Preparation of the flexible image sensor based on vdWs $MAPbI_3$/graphene heterostructure and its application in image recognition. (a, b) Schematic illustration of the as-fabricated flexible (24 × 24) pixels image sensor on PET substrate. (c) Photograph of a flexible image sensor. (d, e) The corresponding output images of a cartoon pig in (d) and QR code of "photodetector" in (e) under an light illumination (30 μW, 633 nm). (f) Schematic illustration of the multicolor imaging systems in human visual system. (g) Schematic diagram of our image sensor showing the vdWs $MAPbI_3$/graphene heterostructure acted as cone cells. (h) The corresponding output image of the flexible image sensor under different light illumination (75 μW, 380, 633 and 750 nm).

Please cite this article as: K. Xia, W. Wu, M. Zhu et al., CVD growth of perovskite/graphene films for high-performance flexible image sensor, Science Bulletin, https://doi.org/10.1016/j.scib.2019.12.015

degradation after repetitive bending at 200 cycles. This finding indicates the excellent operational stability of the vdWs $MAPbI_3$/-graphene heterostructure during repetitive bending tests (Fig. S10 online).

3.4. Preparation and characterization of flexible image sensors based on the vdWs $MAPbI_3$/graphene heterostructure

We also constructed an integrated flexible photodetector array, in which the vdWs $MAPbI_3$/graphene heterostructure acted as cone cells [41]. Fig. 4**a** shows a schematic diagram of the as-prepared flexible photodetector array with (24 × 24) pixels. The size of one pixel is 400 μm × 400 μm. Fig. 4b exhibits a cross-sectional view of the device. The photodetector array consists of six layers, in which polyethylene terephthalate (PET) was used as a flexible substrate. Between the Au (X-direction) and Pt (Y-direction) electrodes, an alumina layer was deposited as an insulating layer to prevent short-circuit. Then, a graphene film was transferred on to the electrode array and patterned, followed by the in-situ growing of $MAPbI_3$ perovskite. The vdWs $MAPbI_3$/graphene heterostructures acted as the light-sensitive materials (see in Materials and method and Figs. S11, S12 (online)). The $MAPbI_3$/graphene of each pixel is almost uniform and can work consistently. The data from all the pixels can be acquired simultaneously by the data acquisition module. Fig. 4c shows the as-prepared flexible photodetector array. We processed two photomasks, including a cartoon pig and QuickMark (QR) code of the word "photodetector" (Fig. 4d and e, respectively) under the illumination wavelength of 633 nm to reveal the imaging capabilities of the device. Excellent image recognition capabilities were observed.

Inspired by the human visual system, we demonstrated the potential of our devices in artificial retina. The human eye has two basic functions: color and shape recognition. We used different illumination wavelengths to examine the color recognition capabilities of the as-prepared device. Fig. 4f shows schematic of the imaging process from the human eye to the visual center of the human brain, where the cone cells in the retina identify the color of the object. Fig. 4g shows the schematic of our image sensor, which is imaged by filtering using three wavelength filters (380, 633, and 750 nm) under white light illumination. The results display that the photocurrent was the largest under 633 nm illumination and smallest under 750 nm, showing great potential for application in artificial visions.

4. Conclusion

In summary, we develop a facile two-step CVD method to synthesize high-quality vdWs $MAPbI_3$/graphene heterostructures by sequentially introducing PbI_2 and MAI with seamless monolayer graphene films as templates. The $MAPbI_3$ layer is composed of ultra-large grain-size $MAPbI_3$ domains and thus exhibits a smooth and dense film. The large-area grain-boundary-free graphene film is used as a template to facilitate the vdWs epitaxial growth of high-quality $MAPbI_3$ film. In the presence of graphene, electrons in the graphene layer are transferred to the proximal hybrid perovskite layer to fill the empty state in the hybrid perovskite valence band produced through photon absorption, thereby reducing the recombination of photoexcited electron-hole pairs in hybrid perovskite. This novel photodetector based on the vdWs $MAPbI_3$/graphene heterostructure shows high photoresponsivity (~10^7 A/W), low operating voltage (0.1 V), and low response time (less than 50 ms). Inspired by the human visual system, we demonstrated the potential of our device in artificial retina, in which the vdWs $MAPbI_3$/graphene heterostructures acted as "cone cells". Our study may open up an avenue to exploit the potential application of high-quality hybrid perovskite heterostructures in optoelectronics, wearable devices, and artificial retina.

Declaration of Competing Interest

The authors declare that they have no conflict of interest.

Acknowledgments

This work was supported by the Ministry of Science and Technology of China (2016YFA0200103), the National Natural Science Foundation of China (51672153, 21975141), and the National Program for Support of Top-notch Young Professionals.

Author contributions

Yingying Zhang and Kailun Xia conceived the idea. Kailun Xia performed most of the experiments. Kailun Xia and Yingying Zhang prepared the draft. Wenqiang Wu, Mengjia Zhu, Zhe Yin, Haomin Wang, Shuo Li, Mingchao Zhang, Huimin Wang, and Haojie Lu participated in part of the experimental and discussed on the results. Caofeng Pan and Anlian Pan instructed the fabrication of the devices. All authors discussed the results and revised the manuscript.

Appendix A. Supplementary materials

Supplementary materials to this article can be found online at https://doi.org/10.1016/j.scib.2019.12.015.

References

[1] Ding J, Fang H, Lian Z, et al. High-performance stretchable photodetector based on $CH_3NH_3PbI_3$ microwires and graphene. Nanoscale 2018;10:10538–44.
[2] Dhanabalan SC, Ponraj JS, Zhang H, et al. Present perspectives of broadband photodetectors based on nanobelts, nanoribbons, nanosheets and the emerging 2D materials. Nanoscale 2016;8:6410–34.
[3] Manga KK, Wang J, Lin M, et al. High-performance broadband photodetector using solution-processible PbSe-TiO_2-graphene hybrids. Adv Mater 2012;24:1697–702.
[4] Ghezzi D, Antognazza MR, Dal Maschio M, et al. A hybrid bioorganic interface for neuronal photoactivation. Nat Commun 2011;2:166.
[5] Lee Y, Kwon J, Hwang E, et al. High-performance perovskite-graphene hybrid photodetector. Adv Mater 2015;27:41–6.
[6] Sun S, Salim T, Mathews N, et al. The origin of high efficiency in low-temperature solution-processable bilayer organometal halide hybrid solar cells. Energy Environ Sci 2014;7:399–407.
[7] Marchioro A, Teuscher J, Friedrich D, et al. Unravelling the mechanism of photoinduced charge transfer processes in lead iodide perovskite solar cells. Nat Photonics 2014;8:250.
[8] Burschka J, Pellet N, Moon S-J, et al. Sequential deposition as a route to high-performance perovskite-sensitized solar cells. Nature 2013;499:316.
[9] Wu W, Wang X, Han X, et al. Flexible photodetector arrays based on patterned $CH_3NH_3PbI_{3-x}Cl_x$ perovskite film for real-time photosensing and imaging. Adv Mater 2019;31:1805913.
[10] Lu J, Carvalho A, Liu H, et al. Hybrid bilayer WSe_2-$CH_3NH_3PbI_3$ organolead halide perovskite as a high-performance photodetector. Angew Chem Int Ed 2016;55:11945–9.
[11] Fang Y, Dong Q, Shao Y, et al. Highly narrowband perovskite single-crystal photodetectors enabled by surface-charge recombination. Nat Photonics 2015;9:679.
[12] Rao H-S, Li W-G, Chen B-X, et al. *In situ* growth of 120 cm^2 CH_3NH_3PbBr 3 perovskite crystal film on FTO glass for narrowband-photodetectors. Adv Mater 2017;29:1602639.
[13] Gao T, Zhang Q, Chen J, et al. Performance-enhancing broadband and flexible photodetectors based on perovskite/ZnO-nanowire hybrid structures. Adv Opt Mater 2017;5:1700206.
[14] Wang JT-W, Ball JM, Barea EM, et al. Low-temperature processed electron collection layers of graphene/TiO_2 nanocomposites in thin film perovskite solar cells. Nano Lett 2014;14:724–30.
[15] Zhu Z, Ma J, Wang Z, et al. Efficiency enhancement of perovskite solar cells through fast electron extraction: the role of graphene quantum dots. J Am Chem Soc 2014;136:3760–3.
[16] Sun Z, Aigouy L, Chen Z. Plasmonic-Enhanced Perovskite-Graphene Hybrid Photodetectors. Nanoscale 2016;8:7377–83.

[17] Niu L, Liu X, Cong C, et al. Controlled synthesis of organic/inorganic van der Waals solid for tunable light-matter interactions. Adv Mater 2015;27:7800–8.
[18] Britnell L, Ribeiro RM, Eckmann A, et al. Strong light-matter interactions in heterostructures of atomically thin films. Science 2013;340:1311–4.
[19] Lopez-Sanchez O, Lembke D, Kayci M, et al. Ultrasensitive photodetectors based on monolayer MoS_2. Nat Nanotechnol 2013;8:497.
[20] Meric I, Han MY, Young AF, et al. Current saturation in zero-bandgap, top-gated graphene field-effect transistors. Nat Nanotechnol 2008;3:654.
[21] Freitag M, Low T, Xia F, et al. Photoconductivity of biased graphene. Nat Photonics 2012;7:53.
[22] Mueller T, Xia F, Avouris P. Graphene photodetectors for high-speed optical communications. Nat Photonics 2010;4:297.
[23] Das Sarma S, Adam S, Hwang EH, et al. Electronic transport in two-dimensional graphene. Rev Mod Phys 2011;83:407–70.
[24] Ge W, Kawahara K, Tsuji M, et al. Large-scale synthesis of NbS_2 nanosheets with controlled orientation on graphene by ambient pressure CVD. Nanoscale 2013;5:5773–8.
[25] Zhang L, Roy SS, Safron NS, et al. Orientation control of selected organic semiconductor crystals achieved by monolayer graphene templates. Adv Mater Interfaces 2016;3:1600621.
[26] Liu X, Balla I, Bergeron H, et al. Rotationally commensurate growth of MoS_2 on epitaxial graphene. ACS Nano 2016;10:1067–75.
[27] Shi Y, Zhou W, Lu A-Y, et al. van der Waals epitaxy of MoS_2 layers using graphene as growth templates. Nano Lett 2012;12:2784–91.
[28] Zhang J, Huang Y, Tan Z, et al. Low-temperature heteroepitaxy of 2D PbI_2/graphene for large-area flexible photodetectors. Adv Mater 2018;30:1803194.
[29] Wang Y, Zhang Y, Lu Y, et al. Hybrid graphene-perovskite phototransistors with ultrahigh responsivity and gain. Adv Opt Mater 2015;3:1389–96.
[30] Patterson AL. The Scherrer formula for X-ray particle size determination. Phys Rev 1939;56:978–82.
[31] Bai F, Qi J, Li F, et al. A high-performance self-powered photodetector based on monolayer MoS_2/perovskite heterostructures. Adv Mater Interfaces 2018;5:1701295.
[32] Li J, Yuan S, Tang G, et al. High-performance, self-powered photodetectors based on perovskite and graphene. ACS Appl Mater Interfaces 2017;9:42779–87.
[33] Pan R, Li H, Wang J, et al. High-responsivity photodetectors based on formamidinium lead halide perovskite quantum dot-graphene hybrid. Part Part Syst Charact 2018;35:1700304.
[34] Dang VQ, Han G-S, Trung TQ, et al. Methylammonium lead iodide perovskite-graphene hybrid channels in flexible broadband phototransistors. Carbon 2016;105:353–61.
[35] Spina M, Lehmann M, Nafradi B, et al. Microengineered $CH_3NH_3PbI_3$ nanowire/graphene phototransistor for low-intensity light detection at room temperature. Small 2015;11:4824–8.
[36] Shao Y, Liu Y, Chen X, et al. Stable graphene-two-dimensional multiphase perovskite heterostructure phototransistors with high gain. Nano Lett 2017;17:7330–8.
[37] Tan Z, Wu Y, Hong H, et al. Two-dimensional $(C_4H_9NH_3)_2PbBr_4$ perovskite crystals for high-performance photodetector. J Am Chem Soc 2016;138:16612–5.
[38] Chang P-H, Liu S-Y, Lan Y-B, et al. Ultrahigh responsivity and detectivity graphene-perovskite hybrid phototransistors by sequential vapor deposition. Sci Rep 2017;7:46281.
[39] Qin L, Wu L, Kattel B, et al. Using bulk heterojunctions and selective electron trapping to enhance the responsivity of perovskite-graphene photodetectors. Adv Funct Mater 2017;27:1704173.
[40] Sun Z, Liu Z, Li J, et al. Infrared photodetectors based on CVD-grown graphene and PbS quantum dots with ultrahigh responsivity. Adv Mater 2012;24:5878–83.
[41] Xue J, Zhu Z, Xu X, et al. Narrowband perovskite photodetector-based image array for potential application in artificial vision. Nano Lett 2018;18:7628–34.

Kailun Xia received his B.S. degree in Materials Science and Engineering from Beijing University of Chemical Technology in 2015. He is currently a Ph.D. candidate at the Department of Chemistry, Tsinghua University, China. His current research is the CVD growth of graphene and its applications in flexible sensors.

Anlian Pan received his Ph.D. degree from the Institute of Physics, Chinese Academy of Sciences in 2006. Afterwards, he worked one year as a Humboldt Research Fellow with Prof. Ulrich Goesele at the Max Planck Institute of Microstructure Physics, and then joined Arizona State University as a postdoctoral fellow, where he became a Research Assistant Professor. He came back to Hunan University and worked as the distinguished Professor of "Furong" Scholar in Hunan Province in 2010. His research interests include the micro-nano optical, electronics of semiconductor nanostructures.

Caofeng Pan received his B.S. degree (2005) and Ph.D. degree (2010) in Materials Science and Engineering from Tsinghua University, China. He then joined the group of Prof. Zhong Lin Wang at the Georgia Institute of Technology as a postdoctoral fellow from 2010 to 2013. He is currently a Professor and a group leader at the Beijing Institute of Nanoenergy and Nanosystems, Chinese Academy of Sciences. His research interests mainly focus on the fields of piezotronics/piezophototronics for fabricating new electronic and optoelectronic devices, nanopower source, hybrid nanogenerators, and self-powered nanosystems.

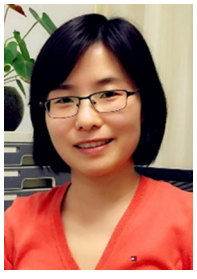

Yingying Zhang received her Ph.D. degree in Physical Chemistry from Peking University in 2007. From 2008 to 2011, she worked in Los Alamos National Laboratory as a Postdoctoral Research Associate. Then, she joined Tsinghua University as an Associate Professor in 2011. Her research focuses on the design and controlled preparation of nanocarbon, silk, and their hybrid materials, aiming to develop high performance flexible electronics and wearable systems.

Please cite this article as: K. Xia, W. Wu, M. Zhu et al., CVD growth of perovskite/graphene films for high-performance flexible image sensor, Science Bulletin, https://doi.org/10.1016/j.scib.2019.12.015